Failure of structures: can you see it coming?

Hinke M. Osinga

Professor, Department of Mathematics, The University of Auckland, Auckland 1142, New Zealand
Email: h.m.osinga@auckland.ac.nz

Abstract

Failure of structures in an earthquake is an important problem that is still not well understood. We investigate how an external force with varying magnitude and principal frequency affects structurural stability. As an example we consider the analytical model of a tied rocking block on an elastic foundation, which exhibits dynamics equivalent to that of a planar, post-tensioned frame on a shake table; here, we consider a periodic external force, but our goal is to predict behaviour of models subject to an aperiodic external force (an earthquake). A standard approach would be to run a large number of simulations over a range of magnitudes and frequencies. We compute the failure boundary directly and find that failure can occur in profoundly different ways. Inherent nonlinearities in the system can have dramatic effects on the stability of the structure, especially when it has a natural frequency close to that of the external forcing.

Keywords: failure boundary; basin of attraction; non-autonomous ordinary differential equation; post-tensioned frame

1 Introduction

The possibility of an earthquake is a constant threat in many countries. For example, New Zealand has recently been experiencing quite a number of earthquakes that resulted in minor to severe damage to buildings. Most notorious is the 2011 Christchurch earthquake, which followed a series of earthquakes starting in September 2010 and provides a striking example of the need for better damage assessment [5]. We certainly like to have buildings that do not collapse during an earthquake. Moreover, it is financially advantageous to design buildings such that virtually no damage is sustained from an earthquake. Ideas for low-damage design include allowing a degree of damage at predefined locations that do not affect the safety of inhabitants [8, 9], and activating rigid body movement of structural members so that forces related to local deformation in the structure will be prevented [1, 2, 4].

Theoretical research into failure of structures often uses a sinusoidal wave as a model for the earthquake. The response of the system is then governed by periodic solutions that have the same period as the sinusoidal earthquake. Such theoretical results provide insight into the system dynamics based on the principal frequency and strength of an earthquake. In this paper, we also consider a sinusoidal external force. We use the model from [2, 7] to illustrate our analysis; this model represents a planar, post-tensioned frame on a shake table and is given by the second-order non-autonomous equation

$$\frac{d^2\varphi}{dt^2} + 2\gamma\,\frac{d\varphi}{dt} + \mu(\varphi) = A\sin(\omega t), \qquad |\,\varphi(t)\,| < \varphi_{\max}. \tag{1}$$

Here, φ is the tilt angle given in units of the critical angle at which the nonlinear stiffness arises. The function $\mu(\varphi)$ is given by

$$\mu(\varphi) = \begin{cases} \varphi, & |\,\varphi| \le 1, \\ \left(\frac{3}{\beta} + \frac{12}{\beta^2} + \frac{8}{\beta^3}\right)\varphi & \\ \quad + \left(3 + \frac{9}{\beta} + 6\frac{1-\sqrt{\psi}}{\beta^2} - 6\frac{\sqrt{\psi}}{\beta^3} - 2\frac{\psi\sqrt{\psi}}{\beta^3\varphi^2}\right)\operatorname{sgn}(\varphi), & |\,\varphi| > 1, \end{cases}$$

where $\psi = (1+\beta)\,(\varphi^2 + \beta\,|\,\varphi\,|)$ and β is the contact-to-cable stiffness ratio; see [2] for details. Solutions φ to (1) are called *admissible* if $|\ \varphi(t)\ | < \varphi_{\max}$ for all t; the maximal tilt angle $\varphi_{\max}$ depends on the characteristics of the building. We use the same parameters as in [2], that is, we fix $\beta = 85$, $\gamma = 0.05$ and $\varphi_{\max} = 10$, and we consider periodic ground motion with frequency $\omega = 0.575$ and varying amplitude A.

For the purpose of this paper, we want to understand how admissibility of the solution $\varphi(t)$ with initial condition $(\varphi(0), \dot\varphi(0)) = (0, 0)$ depends on the forcing amplitude A; we denote this solution by $\Phi_{\mathbf{0}}(t)$. Since the forcing is periodic, any bounded solutions will eventually be periodic and $\Phi_{\mathbf{0}}(t)$ will accumulate onto such a periodic orbit. Consequently, it seems reasonable to expect that it is possible to predict admissibility of $\Phi_{\mathbf{0}}(t)$ from the admissibility of the limiting periodic orbit. In this paper, we argue that such prediction is not possible, not even in an approximating sense. Here, we discuss the case for system (1) with fixed forcing frequency $\omega = 0.575$, but this case is representative for a large class of (nonlinear) systems and a wide range of frequencies.

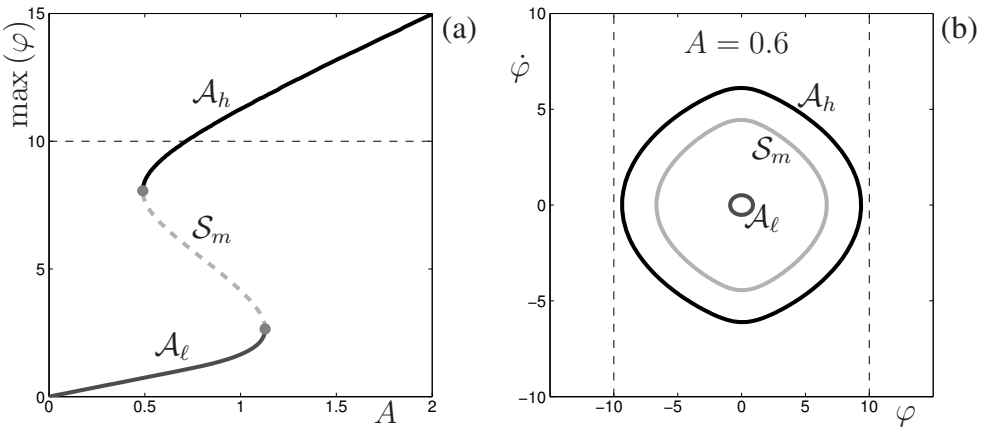

Figure 1: Periodic orbits of system (1) in dependence on the forcing amplitude A. Panel (a) shows A on the horizontal axis and the maximum with respect to φ of the periodic orbit on the vertical axis. Panel (b) shows three co-existing periodic orbits for $A = 0.6$ in the bistable regime plotted in projection onto the $(\varphi, \dot{\varphi})$-plane. The low- and high-amplitude periodic orbits labelled $\mathcal{A}_\ell$ and $\mathcal{A}_h$, respectively, are stable, while the mid-amplitude periodic orbit labelled $\mathcal{S}_m$ is of saddle type.

2 Admissibility of periodic orbits

For a range of pairs (ω, A) in the frequency-amplitude plane, there exist three different periodic orbits and two of these are stable. Such bistability is well known to occur in nonlinear oscillator systems like system (1). One-parameter curves of periodic orbits can readily be computed, for example, via pseudo-arclength continuation in the software package AUTO [3]. Figure 1(a) shows the family of periodic orbits when continuing in A starting from $A = 0$, at which the periodic orbit has zero amplitude and is, in fact, equal to $\Phi_{\mathbf{0}}(t)$. For small A, only one stable periodic orbit $\mathcal{A}_\ell$ exists that has low amplitude and is admissible. The solution $\Phi_{\mathbf{0}}(t)$ accumulates onto $\mathcal{A}_\ell$. We checked that $|\Phi_{\mathbf{0}}(t)| < \varphi_{\max}$ for all t when the forcing is chosen from the regime in the (ω, A)-plane for which only $\mathcal{A}_\ell$ exists. For $A \approx 0.4897$, a fold bifurcation occurs that gives rise to a pair of periodic orbits, an attractor $\mathcal{A}_h$ and a saddle $\mathcal{S}_m$, that have much larger amplitudes than $\mathcal{A}_\ell$. The fold bifurcation marks the beginning of the bistable regime for $\omega = 0.575$ and it lasts until a second fold bifurcation at $A \approx 1.1282$ at which $\mathcal{A}_\ell$ and $\mathcal{S}_m$ merge and disappear. For large A, only $\mathcal{A}_h$ exists and $\Phi_{\mathbf{0}}(t)$ accumulates onto $\mathcal{A}_h$. As indicated in Figure 1(a), the maximum of φ along $\mathcal{A}_h$ exceedes $\varphi_{\max}$ from $A \approx 0.7151$, and $\mathcal{A}_h$ is not admissible for large values of A. Therefore, $\Phi_{\mathbf{0}}(t)$ is not admissible for large A either.

Figure 1(b) shows the co-existence of three periodic orbits for $A = 0.6$ in projection onto the $(\varphi, \dot{\varphi})$-plane. Note the symmetry of these periodic orbits; indeed, any solution φ of system (1) can be transformed into another solution via the transformation $(\varphi, \dot{\varphi}, t) \mapsto (-\varphi, -\dot{\varphi}, t + \pi/\omega)$, which leaves periodic orbits invariant. For $A = 0.6$ all three periodic orbits are admissible and, since $\Phi_{\mathbf{0}}(t)$ converges to $\mathcal{A}_\ell$, the solution $\Phi_{\mathbf{0}}(t)$ is also admissible.

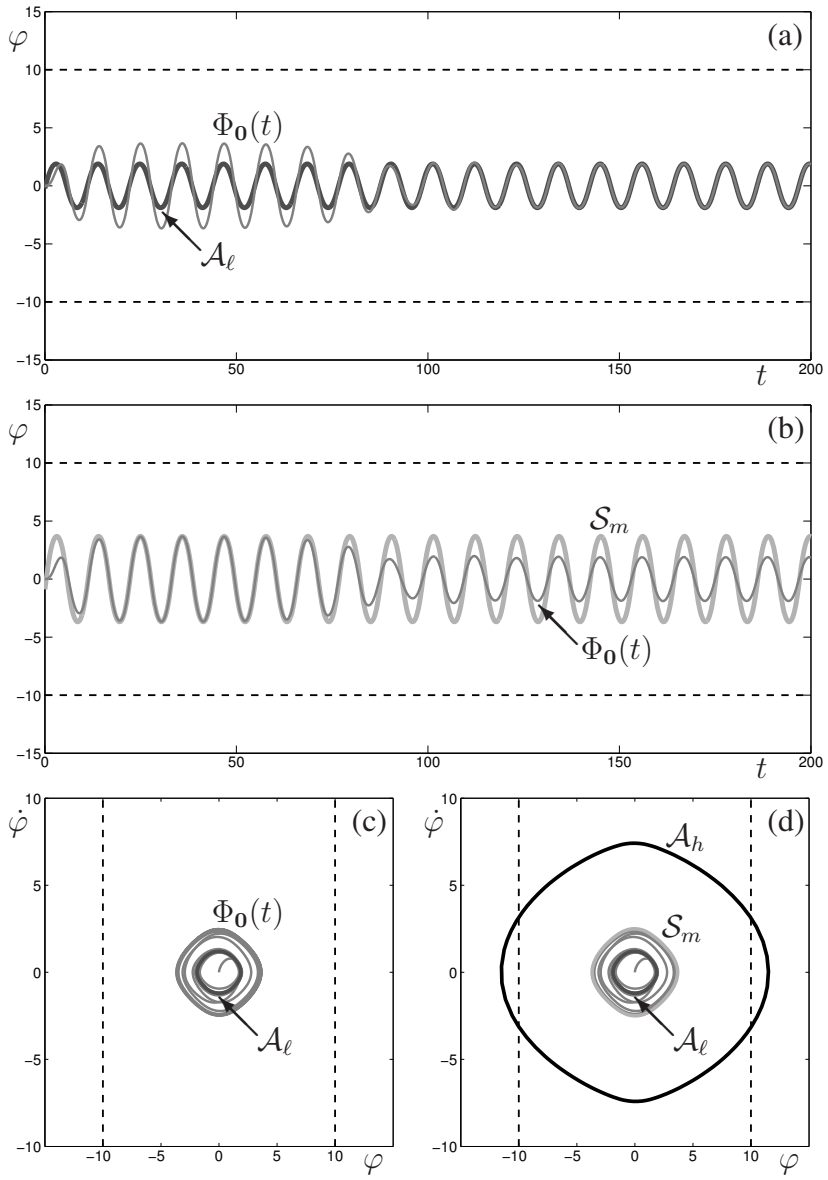

Figure 2: The solution $\Phi_{\mathbf{0}}(t)$ of system (1) with $A = 1.0607$. Panel (a) compares the time series of $\Phi_{\mathbf{0}}(t)$ with that of $\mathcal{A}_\ell$ and panel (b) with that of $\mathcal{S}_m$. The corresponding projections in the $(\varphi, \dot{\varphi})$-plane are shown in panels (c) and (d), respectively.

3 Unexpected failure

Figure 2 shows how $\Phi_{\mathbf{0}}(t)$ behaves as a solution of system (1) compared with the periodic orbits $\mathcal{A}_\ell$, $\mathcal{S}_m$ and $\mathcal{A}_h$ that co-exist for this value of A. The time series of $\Phi_{\mathbf{0}}(t)$ are shown overlayed on $\mathcal{A}_\ell$ in panel (a) and on $\mathcal{S}_m$ in panel (b). Observe in panel (a) that $\Phi_{\mathbf{0}}(t)$ eventually accumulates onto $\mathcal{A}_\ell$, while panel (b) illustrates how $\Phi_{\mathbf{0}}(t)$ visits $\mathcal{S}_m$ before accumulating onto $\mathcal{A}_\ell$. Panels (c) and (d) show the corresponding projections onto the $(\varphi, \dot{\varphi})$-plane, where panel (d) also shows $\mathcal{A}_h$. Even though $\mathcal{A}_h$ is not admissible, the figure gives no reason to expect imminent failure of $\Phi_{\mathbf{0}}(t)$, because $|\,\Phi_{\mathbf{0}}(t)\,|$ is much smaller that $\varphi_{\max}$ for all t.

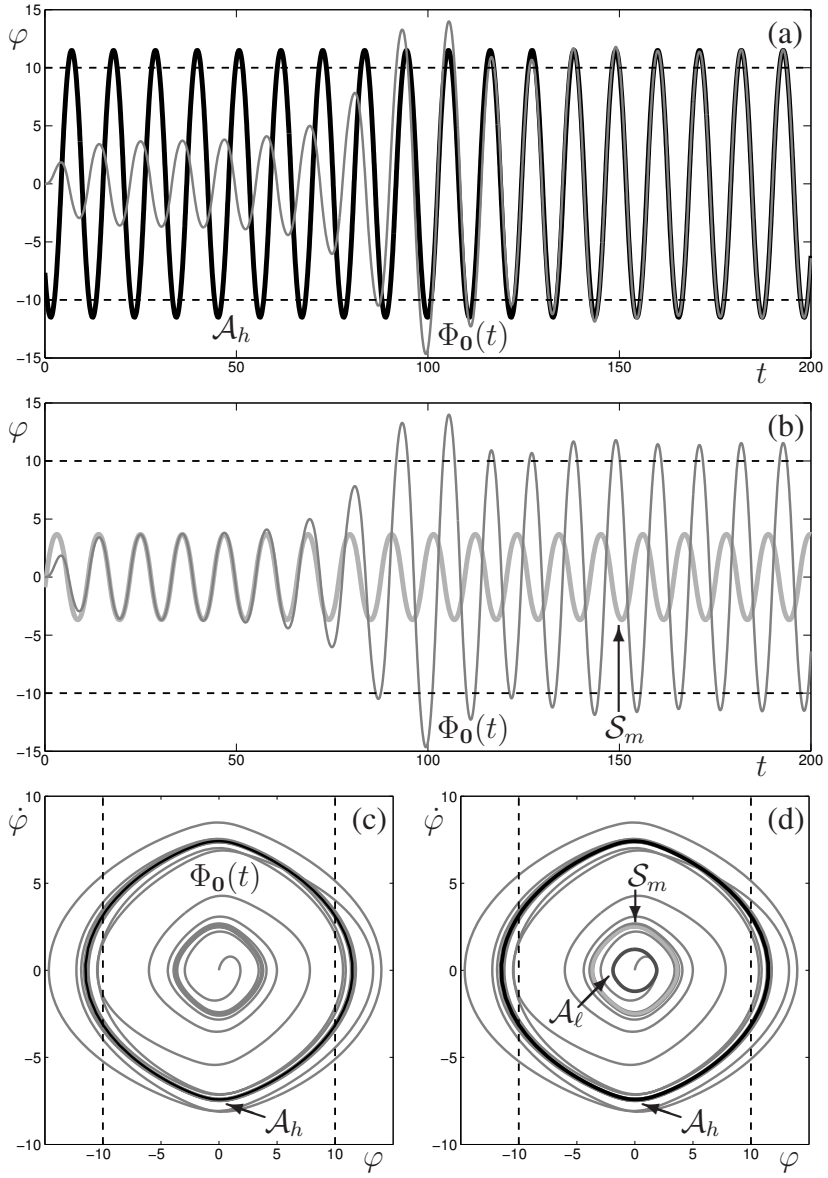

Figure 3: The solution $\Phi_{\mathbf{0}}(t)$ of system (1) with $A = 1.0610$. Panel (a) compares the time series of $\Phi_{\mathbf{0}}(t)$ with that of $\mathcal{A}_h$ and panel (b) with that of $\mathcal{S}_m$. The corresponding projections in the $(\varphi, \dot{\varphi})$-plane are shown in panels (c) and (d), respectively.

However, $\Phi_{\mathbf{0}}(t)$ already fails when $A = 1.0610$. The behaviour of $\Phi_{\mathbf{0}}(t)$ for this slightly larger value of A is shown in Figure 3. The figure is similar to Figure 2, showing the time series of $\Phi_{\mathbf{0}}(t)$ in panels (a) and (b) and the corresponding phase portraits in the $(\varphi, \dot{\varphi})$-plane in panels (c) and (d). As in Figure 2, the solution $\Phi_{\mathbf{0}}(t)$ again visits $\mathcal{S}_m$ initially, but then $\Phi_{\mathbf{0}}(t)$ accumulates onto $\mathcal{A}_h$ instead of $\mathcal{A}_\ell$. Since $\mathcal{A}_h$ is not admissible, admissibility of $\Phi_{\mathbf{0}}(t)$ is also lost at this A-value. However, observe from Figure 3 that failure of $\Phi_{\mathbf{0}}(t)$ occurs for relatively large t and the initial tracking of $\mathcal{S}_m$ is extremely similar to the admissible response in Figure 2. The transition from accumulation onto $\mathcal{A}_\ell$ to accumulation onto $\mathcal{A}_h$ occurs well after $\mathcal{A}_h$ loses admissibility, but before the fold bifurcation at which $\mathcal{A}_\ell$ and $\mathcal{S}_m$ disappear.

4 Conclusions

We estimate the precise A-value at which $\Phi_{\mathbf{0}}(t)$ fails to be $A \approx 1.06076447$. At this value, $\Phi_{\mathbf{0}}(t)$ accumulates onto $\mathcal{S}_m$ instead of $\mathcal{A}_\ell$ or $\mathcal{A}_h$. Such behaviour is special, because $\mathcal{S}_m$ is not attracting. It means that $\Phi_{\mathbf{0}}(t)$ is contained in the stable manifold of $\mathcal{S}_m$, which is a surface in $(\varphi, \dot{\varphi}, t)$-space that separates the basins of attraction of $\mathcal{A}_\ell$ and $\mathcal{A}_h$. As illustrated in Figures 2 and 3, just before and just after loss of admissibility, respectively, it is very hard to predict this type of failure.

From a mathematical point of view, the failure described in this paper can be characterised as the precise moment when $\Phi_{\mathbf{0}}(t)$ is contained in the stable manifold of $\mathcal{S}_m$. Using advanced numerical techniques [6], it is possible to approximate the exact (ω, A)-pairs at which such an event occurs. The algorithmic approach is based on pseudo-arclength continuation of a two-point boundary value problem, which is reminiscent of the computational approach described in [7] and much more challenging than the method for finding the curve of periodic orbits shown in Figure 1(a). Full details of such a computational approach will be presented elsewhere.

Of course, earthquakes are not periodic and the precise behaviour of $\Phi_{\mathbf{0}}(t)$ when subjected to a general external force is harder to analyse. However, it is plausible to expect underlying attracting motion that plays the same role as $\mathcal{A}_\ell$ and $\mathcal{A}_h$, which means that there must also exist saddle-type motion similar to $\mathcal{S}_m$. An appropriate characterisation of the failure as described here for periodic forcing remains a challenging direction for future research.

Acknowledgments

My special thanks to Chris Budd for helpfull discussions on the geometry of the failure boundary.

References

[1] Acikgoz, S. and De Jong, M.J. (2012) The interaction of elasticity and rocking in flexible structures allowed to uplift, *Earthquake Engineering and Structural Dynamics* Vol **41**, No 15, pp 2177–2194.

[2] Alexander, N. A., Oddbjornsson, O., Taylor, C. A., Osinga, H. M. and Kelly, D. E. (2011) Exploring the dynamics of a class of post-tensioned, moment resisting frames, *Journal of Sound and Vibration* Vol **330**, No 15, pp 3710–3728.

[3] Doedel, E. J. (2007) AUTO-07P: Continuation and bifurcation software for ordinary differential equations, with major contributions from Champneys, A. R., Fairgrieve, T. F., Kuznetsov, Yu. A., Oldeman, B. E., Paffenroth, R. C., Sandstede, B., Wang, X. J. and Zhang, C.; available at `http://cmvl.cs.concordia.ca/auto/`

[4] Fardis, M.N. and Rakicevic, Z.T. (2012) *Role of Seismic Testing Facilities in Performance-Based Earthquake Engineering: SERIES Workshop* Springer-Verlag, Dordrecht, Heidelberg, London, New York.

[5] Kam, W.Y., Pampanin, S. and Elwood, K. (2011) Seismic performance of reinforced concrete buildings in the 22 February Christchurch (Lyttelton) earthquake, *Bulletin of the New Zealand Society for Earthquake Engineering* Vol **44**, No 4, pp. 239–278.

[6] Krauskopf, B. and Osinga, H. M. (2007) Computing invariant manifolds via the continuation of orbit segments, in Krauskopf, B., Osinga, H. M. and Galán-Vioque, J. (eds.), *Numerical Continuation Methods for Dynamical Systems*, Springer-Verlag, Berlin, pp 117–154.

[7] Osinga, H. M. (2014) Computing failure boundaries by continuation of a two-point boundary value problem, in Proceedings of the 9th International Conference on Structural Dynamics, EURODYN 2014, Porto #MS10-263, pp 1891–1897.

[8] Priestley, M. J. N., Sritharan, S., Conley, J. R. and Pampanin, S. (1999) Preliminary results and conclusiongs from the PRESSS five-story precast concrete test building, *PCI Journal* Vol **44**, No 6, pp 42–67.

[9] Qin, X., Chen, Y. and Chouw, N. (2013) Effect of uplift and soil nonlinearity on plastic hinge development and induced vibrations in structures, *Advances in Structural Engineering* Vol **16**, No 10, pp 135–147.